Edge-based Compression and Classification for Smart Healthcare Systems: Concept, Implementation and Evaluation

Edge-based Compression and Classification for Smart Healthcare Systems: Concept, Implementation and Evaluation

Alaa Awad Abdellatif [a,c], Ahmed Emam [b]
Carla-Fabiana Chiasserini [c], Amr Mohamed [a], Ali Jaoua [a], and Rabab Ward [d]

[a] *Department of Computer Science and Engineering, Qatar University, Qatar*

[b] *School of Computer Science, Carnegie Mellon University, Qatar*

[c] *Department of Electronics and Telecommunications, Politecnico di Torino, Torino, Italy*

[d] *Electrical and Computer Engineering Department, University of British Columbia, Vancouver, Canada*

Abstract

Smart healthcare systems require recording, transmitting and processing large volumes of multimodal medical data generated from different types of sensors and medical devices, which is challenging and may turn some of the remote health monitoring applications impractical. Moving computational intelligence to the network edge is a promising approach for providing efficient and convenient ways for continuous-remote monitoring. Implementing efficient edge-based classification and data reduction techniques are of paramount importance to enable smart healthcare systems with efficient real-time and cost-effective remote monitoring. Thus, we present our vision of leveraging edge computing to monitor, process, and make autonomous decisions for smart health applications. In particular, we present and implement an accurate and lightweight classification mechanism that, leveraging some time-domain features extracted from the vital signs, allows for a reliable seizures detection at the network edge with precise classification accuracy and low computational requirement. We then propose and implement a selective data transfer scheme, which opts for the most convenient way for data transmission depending on the detected patient's conditions. In addition to that, we propose a reliable energy-efficient emergency notification system for epileptic seizure detection, based on conceptual learning and fuzzy classification. Our experimental results assess the performance of the proposed system in terms of data reduction, classification accuracy, battery lifetime, and transmission delay. We show the effectiveness of our system and its ability to outperform conventional remote monitoring systems that ignore data processing at the edge by: (i) achieving 98.3% classification accuracy

for seizures detection, (ii) extending battery lifetime by 60%, and (iii) decreasing average transmission delay by 90%.

Key words: Edge computing, conceptual learning, feature extraction, fuzzy classification, wavelet compression.

---

1 Introduction

The rising evolution of computational intelligence systems, mobile communications, and Internet of Medical Things (IoMT) has boosted the evolution of traditional healthcare processes into smart health services. It is a fact that many elder patients need continuous-remote healthcare monitoring. Thus, such advances in Body Area Sensor Network (BASN), and smart healthcare systems will allow remote real-time monitoring of patients without constraining their activities (Patel & Wang, 2010).

In this paper, we focus on mobile-health monitoring system for brain disorders and, in particular, we propose an energy-efficient remote monitoring system for epileptic seizure detection [1]. Electroencephalography (EEG) signal plays an important role in the diagnosis of epileptic disease, brain death, tumors, stroke and several brain disorders (Adeli, Ghosh-Dastidar, & Dadmehr, 2007). Such applications typically require the recording, transmission, and processing of very large volumes of data. Consider, for instance, high-quality EEG devices consisting of up to 100 electrodes, each one working at sampling rate as high as 1000 samples/s. By representing each sample by 2 bytes, it results in a data rate of 1.6 Mbps per single patient. Also, in normal conditions, information about medical patients should be reported to the MHC every 5 minutes, while, in the case of emergency where high-intensive monitoring is needed, all data collected by the BASN should be reported every 10 seconds (Yuce, Ng, Myo, Khan, & Liu, 2007). The wireless transmission of such amount of data is highly energy consuming (it amounts to about 70% of the total power consumption of a wireless EEG monitoring system (Yazicioglu et al., 2009)); also, it requires significant processing capabilities, high reliability and, in the case of emergency, very short latency.

Such requirements cannot be supported by resource-constrained Personal/Patient Data Aggregator (PDA), unless we adopt a smart solution. The conventional mobile-health system using simple sensor-to-cloud architecture (Kraemer, Braten, Tamkittikhun, & Palma, 2017), where the raw date is collected from different sensor nodes and send to the cloud for processing, becomes unsuitable for smart-health (s-health). Such centralized approach cannot provide sufficient scalability and responsiveness while causing heavy network loads. On the contrary, leveraging edge computing capabilities, s-health systems can significantly improve medical data delivery while decreasing the latency and energy consumption.

Email addresses: aawad@qu.edu.qa (Alaa Awad Abdellatif), aemam@cs.cmu.edu (Ahmed Emam), chiasserini@polito.it (Carla-Fabiana Chiasserini), amrm@qu.edu.qa (Amr Mohamed), jaoua@qu.edu.qa (Ali Jaoua), rababw@ece.ubc.ca (Rabab Ward).

[1] Epilepsy is the most common neurological disorder in the world after stroke and Alzheimer's disease. It is estimated to affect more than 65 million people worldwide, with more than 80% of people with epilepsy living in developing countries (Thurman et al., 2011).

Thus, given the requirements and constraints of remote monitoring systems, our goal is to enable energy-efficient delivery of real-time medical data through implementing: (i) a mechanism for abnormal pattern detection at the network edge that allows us to identify the patient's state, and (ii) a selective transfer scheme that, exploiting the above detection mechanism, transmits toward the Mobile-Health Cloud (MHC) only the data that is necessary based on the current situation. Motivated by the edge computing paradigm, where we push the computational intelligence closer to the patient, we propose and implement s-health system, shown in Fig. 1, for detecting patient's state that exploits feature extraction and fuzzy classification at the network edge. Then, depending on the patient's state, our s-health system can exploit different data reduction techniques, in order to reduce the amount of transmitted data, hence, improve the cost of delivering vital signs to the MHC, in terms of, detection and transmission latency, as well as transmission energy consumption and monetary cost.

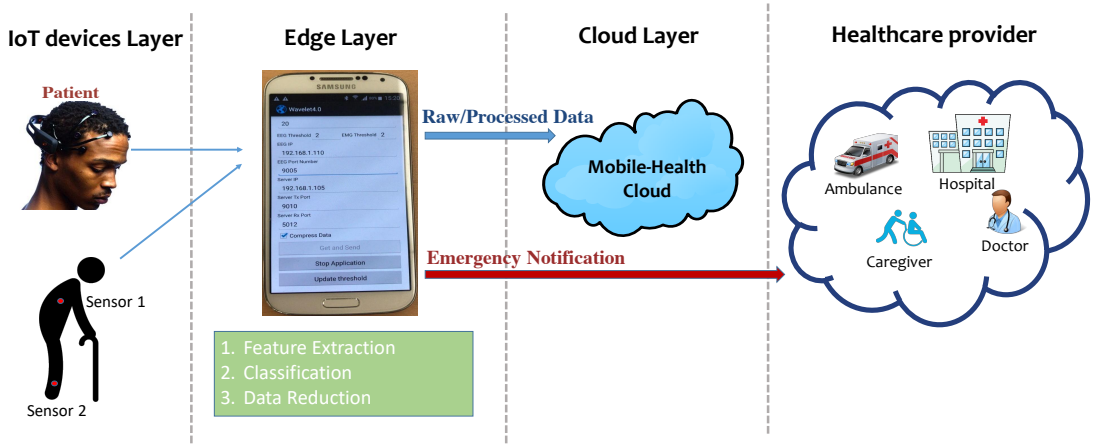

Fig. 1. The proposed s-health system architecture.

The rest of the paper is organized as follows. Section 2 discusses the related work while highlighting the novelty of our study. Section 3 presents the system model. Section 4 introduces the techniques for feature extraction and selection. Section 5 describes the proposed swift in-network classification scheme. Data transfer, along with our solution for adaptive data compression, is introduced in Section 6, while Section 7 presents the implementation of the proposed s-health system. Section 8 introduces our performance evaluation. Finally, Section 9 concludes the paper.

2 Related Work

The rapid growth of IoMT has motivated the development of innovative applications for information intensive fields such as healthcare services (Xu et al., 2014). The conventional cloud computing architecture facilitates for the smart devices (e.g., sensors, smartphones) to exchange information with the cloud through 3G/4G technologies, or IoT gateway (Sheng, Mahapatra, Zhu, & Leung, 2015). Thus, on one hand provides uniform, concise, and scalable processing as well as storage services for supporting application requirements. On the other hand, the deployments of remote health monitoring, emergency response, and in general delay-sensitive IoT applications on the cloud are facing challenges. For instance, the delay caused by transferring data to and from the cloud to the application is unpredictable, in addition to the economic considerations, technical limitations, and administrative issues (Sarkar & Misra, 2016). In (Menshawy, Benharref, & Serhani, 2015), the authors implement an automatic mobile-based

health system exploiting the information contained in EEG signals for seizures detection. This system consists of back-end part (i.e., server part) and front-end part (i.e., mobile part). Server part comprises the pre-processing task, which includes feature extraction, normalization, and selection, as well as classification task. While mobile part includes data acquisition, visualization, and transmission. The authors in this study also present different algorithms in the pre-processing and classification stages to implement a reliable system in terms of execution time and classification accuracy. However, they consider the mobile part as a communication hub, while moving the pre-processing and classification tasks to the server. Considering such centralized approach cannot provide a sufficiently high level of scalability and responsiveness given the limited bandwidth availability, energy consumption, and data privacy concerns. On the contrary, processing and compressing the gathered data at the mobile edge greatly reduces the amount of information to be transferred toward the cloud, hence the bandwidth and energy consumption, while ensuring privacy protection.

To address the aforementioned challenges, Edge computing and Fog computing were proposed to use computing resources near IoMT devices for local storage and preliminary data processing (Dastjerdi & Buyya, 2016). In this context, the authors in (Pace et al., 2018) proposed a software framework for healthcare applications based on Edge paradigm. This framework is used for acquiring and analyzing Heart Rate Variability (HRV) signals, while presenting the advantages of leveraging Edge paradigm rather than the classical Cloud paradigm. The authors in (Cerina, Notargiacomo, Paccanit, & Santambrogio, 2017) discuss the benefits of fog architectures in preventive healthcare applications, and the feasibility of Field-Programmable Gate Array (FPGA) technology in implementing efficient Fog nodes. This aforementioned work motivate that performing efficient in-network processing with feature extraction and adaptive compression at the edge would significantly assist in network congestion, offload core network traffic, accelerating analysis, and meeting application requirements for swift and secure data transfer.

Most of the related work in the context of Wireless Sensor Network (WSN) was motivated by the reduction of latency to perform classification at the sensor network. Machine learning methods have been investigated to exploit historical data and improve the performance of sensor networks through discovering important correlations in the sensor data and propose improved sensor deployment for maximum data coverage. For instance, the authors in (Rossi, Krishnamachari, & Kuo, 2016) present a classification technique for efficient data collection in WSN. However, it is assumed that the end users are interested only in rounds of measurements characterized by certain patterns. Hence, the WSN exploits the classification with the goal of selecting most relevant rounds of gathered data in order to reduce the amount of transmitted data. A comprehensive overview of recent machine learning methods applied in WSN can be found in (Alsheikh, Lin, Niyato, & Tan, 2014). However, many of the aforementioned works performing classification at the sensor network focused on the reduction of latency rather than energy efficiency. It is not clear whether that is more energy efficient than transmitting and classifying the data at the end users or not, since such classification techniques require distributed feature extraction and transmission, which may be less or more energy consuming than the transmission of measurements without classification. Furthermore, learning by examples needs to process large datasets to ensure high accuracy, whereas it is not straightforward to mathematically formulate the learned model, or to have the full control over the knowledge discovery process

Fuzzy logic techniques have been also investigated in the area of patients' care to predict and categorize patients status (Cosenza, 2012)(Tatari, Akbarzadeh, & Sabahi, 2012). For instance, the author in (Cosenza, 2012) leverages fuzzy techniques in the development of a decision

support system that optimizes the postprandial glycemia in type 1 diabetes patients, while the authors in (Tatari et al., 2012) exploit fuzzy and probabilistic computing to assess breast cancer risk. In (Al-Dmour, Sagahyroon, Al-Ali, & Abusnana, 2017), the authors discuss the design and implementation of a fuzzy logic-based warning system that exploits fuzzy logic to categorize patients status and send timely warning messages to healthcare service providers. In (Castanho, Hernandes, R, Rautenberg, & Billis, 2013), a fuzzy expert system is developed to classify the patients with confined or non-confined prostate cancer showing the efficiency of the presented fuzzy system compared with other probabilistic systems.

The enormous advances in smartphone capabilities has also motivated the development of smartphone applications (apps) for healthcare monitoring. Leveraging built-in sensors of the mobile phone, smartwatch, gyroscopic sensors, and GPS module has enabled developing different apps for seizures detection at the smartphone. For instance, "Epdetect" application employs signal processing techniques to differentiate between normal movements and those associated with seizures ("Epilepsy Detector Application", 2017). When any abnormal movements are detected, this app triggers seizures detected alarm. Seizario (Helmy & Helmy, 2015) is another mobile app that uses only smartphone to detect seizures convulsions and falls exploiting accelerometer-based learning algorithms with elaborate finite-state-machines. However, such apps that relay on movements detections instead of the analysis of EEG signals are not reliable for detecting absence seizures that does not result in convulsions.

Accordingly, leveraging higher levels of autonomy and intelligence at the edge through moving processing and classification tasks to the mobile edge will significantly enhance energy consumption, privacy protection, as well as latency and response time, while satisfying the requirements of smart healthcare services. In this context, our main contributions can be summarized as follows.

(1) We design an energy-efficient s-health system for epileptic seizure detection and notification, which adapts the type of information to transmit over the wireless channel based on the patient's state. In the proposed s-health system, local in-network processing at the edge is executed on the raw EEG data before their transmission. Thus, we can accurately estimate the patient's state. Then, if no active seizures is detected, data can be either compressed or further processed to extract and transmit only those features of the signal that are pertinent to the patient's state assessment.
(2) We apply feature extraction to EEG data and exploit such features to develop a fuzzy classification technique. Our classifier, named Swift In-network Classification (SIC), allows for a very accurate detection of the patient's state, which ensures a quick notification about the patient's state at the PDA, as well as at the remote server (doctor's machine). Also, the mechanism we propose provides a quick response while keeping the complexity low, thus it is amenable for implementation at the mobile edge (PDA).
(3) We present a comparative study of frequency-domain and time-domain feature extraction techniques, discussing the tradeoff that they exhibit in terms of transmitted data length and classification accuracy.
(4) We implement a remote real-time EEG monitoring system, which is composed of a wearable EEG device that connects to smartphone (PDA) via WiFi. The PDA handles the EEG readings via a specific cellphone application we have developed, and applies proposed SIC technique for detecting the patient's state. Based on the detected status, the PDA transmits the appropriate data type to a remote server, while in case of emergency, an emergency notification is declared at the PDA and forwarded to the server. At the server, the transmitted data from PDA is received, and a real-time data reconstruction and dis-

tortion evaluation for the compressed-received data is applied. We have tested this system using online and offline data, where the online data representing the normal EEG signal that is collected from the wearable device and forwarded to the PDA for processing. The offline data is leveraged through implementing a data emulator application to simulate patients with active epileptic seizure.

3 System Model

We focus on epileptic seizure detection as an application of EEG-based diagnosis. Recent studies have indeed shown that the dynamic properties of EEG signals can be effectively used to differentiate between healthy subjects and diagnosed patients with epileptic disease. In particular, we consider the wireless EEG telemonitoring system, shown in Fig. 1, which is organized in a three-tier (i.e. cloud/edge/IoT devices) architecture that provides the gathered data/emergency notification to the healthcare provider. In this architecture, the EEG data is collected from a patient using an EEG headset in the IoT devices layer. Then, it is periodically transferred to a PDA, i.e., a smartphone, that represents the Edge Layer, which processes the gathered data and forwards the processed data to the far cloud, hereinafter referred to as Mobile-health Cloud (MHC).

We remark that our study does not only focus on monitoring people who suffer from active epilepsy, but also consider normal people who are more susceptible to seizures (i.e., high risk people). For instance, people who have surgery and became seizures free are able to stop seizures medicine. However, they may need to stay on monitoring to prevent seizures from coming back, even after becoming normal (Berg AT et al., 2001). Also, seizures do happen frequently in people who have had a traumatic injury to the brain. Most seizures occur in the first several days or weeks after the brain injury, however some cases may appear months or years after the injury (Englander & Jeffrey et al, 2014). Thus, it is of prominent importance to monitor such high risk people for seizures.

In this context, in order to conduct our study, we leverage the EEG database in (Andrzejak et al., 2001) considering three classes of patients: seizure-free (SF), non-active (NAC), and active (AC). The first one includes seizure-free subjects (i.e., do not have seizures), the second refers to non-active patients diagnosed with epileptic disorder, however they are in non-active state, while the third class comprises patients with active epileptic seizure, as shown in Fig. 2. Each class includes 100 single-channel EEG segments (i.e., 100 rows), and, given a sensing time frame of 23.6 s and a sampling rate of 173.6 sample/s, for each channel there are 4096 samples (i.e., columns).

With the aim to develop an energy-efficient monitoring system, we design a mechanism that enables a PDA to always select the most appropriate configuration for transmitting the patient's information, based on the patient's state. The proposed scheme is depicted in Fig. 3.

Starting from the collected EEG data, the PDA first derives specific values (features) that are informative, non-redundant, and pertinent to seizures detection. These features allow the classification process at the PDA (i.e., the mobile edge), as well as at the MHC when necessary, leading to an accurate interpretation of the patient's state. Based on the detected patient's state, the PDA will act as follows:

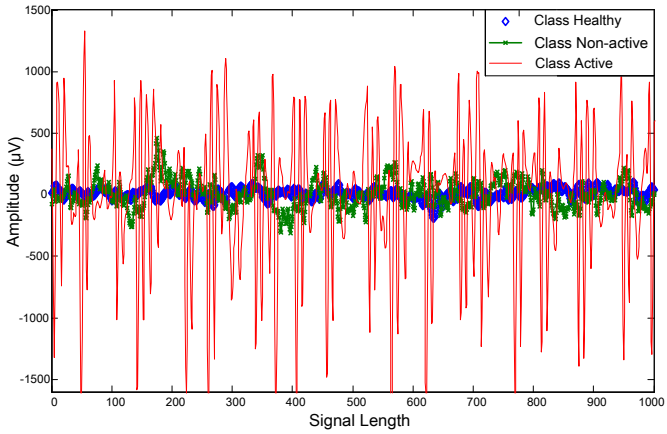

Fig. 2. Representation of the three classes of EEG signals in the time domain.

- in case of AC (i.e., of an emergency), it will send toward the healthcare service provider an Emergency Notification (EN) signal, along with raw EEG data to the MHC for high-intensive monitoring;
- in case of NAC, it will compress and, then, forward EEG data;
- in case of SF, it will send only EEG features (i.e., frequency-domain or time-domain features).

At the MHC, according to the received data, signal reconstruction, feature extraction, classification, or distortion evaluation can be performed, in order to accurately evaluate the state of the patient.

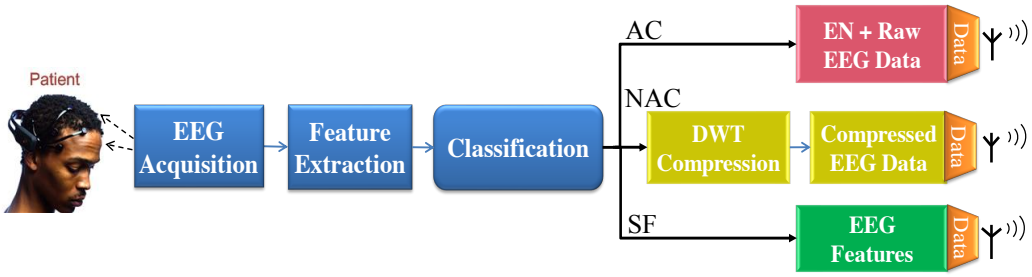

Fig. 3. Proposed in-network processing tasks at the edge.

It is worth mentioning that for SF it is important to monitor patient's state through sending EEG features to confirm the status stability, whereas sending raw or compressed signal will not add much information to the physicians as long as the state is stable (no further analysis is needed in this case). While for NAC, it is important for the physicians to analyze the EEG signal not only the features, so they can expect when seizures could happen. Thus, it is worth to send the compressed data with acceptable level of distortion to the MHC. We also highlight that the main modules required at the PDA to successfully implement the above scheme, are: amplifier and sampling, Discrete Wavelet Transform (DWT) compression, Feature Extraction (FE) components, quantization, encoding, and RF transmission modules.

4 Feature Extraction

Our first step toward the design of a reliable, yet energy-efficient, system for epileptic seizure detection and notification, consists in identifying a set of epileptic-related features, and apply

feature extraction on the raw data collected at the PDA level. To this end, here we present two possible approaches: time-domain and the frequency-domain feature extraction.

4.1 Time-Domain Feature Extraction (TD-FE)

Our goal is to select the most representative time features that can be used to distinguish between different EEG classes. As shown by the signal behavior in Fig. 2, the three classes under study exhibit different mean and variance values, as well as different amplitude variations over time. To account for the latter, it is crucial to consider as relevant feature the waveform length, as a representation of the signal variation over time, i.e., the cumulative length of the waveform over a given time window. In addition, Auto-regression (AR) coefficients should be recorded as they provide a smooth and compact representation of the signal spectrum. We therefore select the following four statistical features:

Mean absolute value

$$\mu_j = \frac{\sum_{k=1}^{N} |x_j(k)|}{N} \tag{1}$$

Variance

$$\sigma_j^2 = \frac{\sum_{k=1}^{N} x_j^2(k)}{N-1} \tag{2}$$

Waveform length

$$WL_j = \sum_{k=1}^{N-1} |x_j(k+1) - x_j(k)| \tag{3}$$

Auto-regression coefficients

$$x_j(k) = \sum_{i=1}^{p} a_i x_j(k-i) + e_k \tag{4}$$

where:

- N is the considered time window expressed in number of samples, namely $N = 4096$ samples,
- $x_j(k)$ is the k-th sample, $k \in \{1, .., N\}$, referring to the generic patient j,
- a_i represents the auto-regression coefficient, p is the order of the auto-regression model, and e_k is the residual white noise (Phinyomark, Limsakul, & Phukpattaranont, 2009).

Accordingly, for a given patient, the above four time features will be representative of the patient's state over a time window of N samples.

4.2 Frequency-Domain Feature Extraction (FD-FE)

In this case, we first transform the gathered EEG signal into the frequency domain using the Fast Fourier Transform (FFT) (Proakis & Manolakis, 2007), which has a complexity of $O(N \log N)$. In the frequency domain, we observe that the different EEG classes have different amplitude range (see Fig. 4) – an important characteristic that significantly facilitates discrimination between the different classes.

The frequency spectrum of the EEG signal is therefore segmented into multi-subbands, each of which includes a certain number of frequency components. Different subsets of these sub-bands

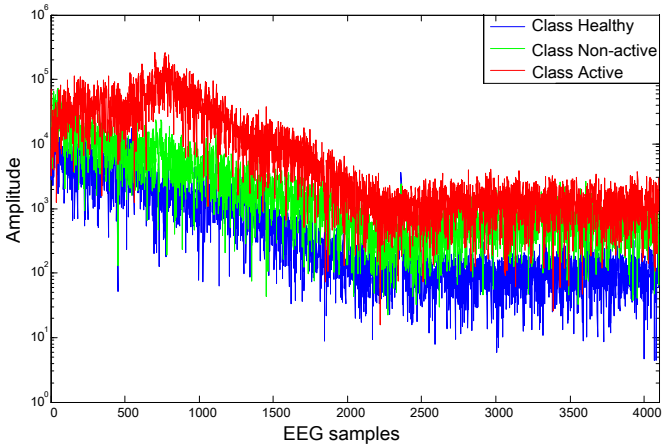

Fig. 4. The three classes of EEG signal after FFT.

can then be selected as feature vector (Ahirwal & londhe, 2012). Specifically, we use the following five frequency sub-bands, named α, β, δ, γ, and θ, corresponding to the frequency ranges $8-12$, $12-32$, $0.2-3$, >32, and $3-8$ Hz, respectively (Hussein, Mohamed, & Alghoniemy, 2015a). Clearly, the more the frequency subsets that we consider, the larger the amount of data to be processed (and then transmitted), which in turn increases the energy consumption while providing higher classification accuracy.

5 Swift In-network Classification

We now present the second step toward a reliable, energy-efficient detection and notification of epileptic seizure: classification of the patient's state. Specifically, we leverage the feature extraction techniques described above, and then use fuzzy classification to detect EEG patterns at the mobile edge. As mentioned before, such classification, named SIC (Swift In-network Classification), allows the PDA to select the most suitable transmission option given the detected state of the patient, i.e., to transfer to the MHC only features, compressed data, or all raw data.

In what follows, we first review some basic definitions from relational algebra as well as Formal Concept Analysis (FCA), for analyzing data and formally representing conceptual knowledge. Then we introduce an automated method to transform EEG signal into a fuzzy binary relation. The resultant relation is decomposed into a set of optimal concepts to build association rules for a fast, yet accurate, classification.

5.1 Using Knowledge Discovery in EEG Datasets

We start by introducing the basic notions used to induce a crisp relation from a fuzzy one (Maddouri, Elloumi, & Jaoua, 1998), and to create a set of association rules from the obtained crisp relation (Alja'am et al., 2006). Let $\mathcal{O}$ be the set of patients (i.e., objects) and $\mathcal{P}$ the set of features (i.e., properties). The fuzzy relation on the universe $\mathcal{U} = \mathcal{O} \times \mathcal{P}$ measures the strength of the correlation between patients and features. In order to proceed further, we recall the following formal definitions (Dubois & Prade, 2000)(Novak, 1989):

Definition 1. A fuzzy binary relation, R, on the universe $\mathcal{U} = \mathcal{O} \times \mathcal{P}$, is a fuzzy set defined

on $\mathcal{U}$, such that for any given pair (o, p), where $o \in \mathcal{O}, p \in \mathcal{P}$, $\mu_R(o, p)$ is the value of the membership function within R, representing the strength of relation between o and p.

Definition 2. Let $\alpha \in [0, 1]$. The α-cut of R, denoted by R_α, is a crisp binary relation such that, for all $(o, p) \in \mathcal{U}$, $\mu_{R_\alpha}(o, p) = 1$, if $\mu_R(o, p) \geq \alpha$. Else, $\mu_{R_\alpha}(o, p) = 0$.

Definition 3. A rectangle of R_α, denoted by $(\mathcal{A}, \mathcal{B})$, is a Cartesian product of two subsets $\mathcal{A} \subseteq \mathcal{O}$, $\mathcal{B} \subseteq \mathcal{P}$, such that $\mathcal{A} \times \mathcal{B} \subseteq R_\alpha$.

Definition 4. A rectangle $(\mathcal{A}, \mathcal{B})$ is said to be maximal under relation R_α if $\mathcal{A} \times \mathcal{B} \subseteq \hat{\mathcal{A}} \times \hat{\mathcal{B}} \subseteq R_\alpha \Rightarrow \mathcal{A} = \hat{\mathcal{A}}$ and $\mathcal{B} = \hat{\mathcal{B}}$.

Definition 5. A maximal rectangle $(\mathcal{A}, \mathcal{B})$ is said to be optimal if it maximizes the gain function. The gain function of a rectangle $(\mathcal{A}, \mathcal{B})$ is given by: $G(\mathcal{A}, \mathcal{B}) = |\mathcal{A}| \cdot |\mathcal{B}| - (|\mathcal{A}| + |\mathcal{B}|)$ where $|\cdot|$ denotes the set cardinality.

Definition 6. The coverage of R_α is defined as a set of optimal rectangles $\mathcal{V}$ under R_α such that any element $(a, b) \in R_\alpha$ is included in at least one rectangle of $\mathcal{V}$.

Examples illustrating the above definitions can be found in (Maddouri et al., 1998)(Sarfraz, 2005).

As mentioned, in our case R represents the correlation between patients and features, which can be transformed into a crisp binary relation, R_α, by setting a proper value for the threshold α. Thus, an optimal rectangle corresponds to the maximum number of patients that share the maximum number of features can be obtained. Our aim is to obtain the minimal set of optimal rectangles covering our binary relation.

To this end, given R_α, we adopt the decomposition of a binary relation presented in (Khcherif, Gammoudi, & Jaoua, 2000), which is based on difunctional decomposition. Accordingly, first the Fringe Relation of a binary relation is calculated. This fringe relation is, by definition, a difunctional relation, and all its elements are isolated points. If (a, b) is an isolated point, by definition it is included in one maximal rectangle only (Khcherif et al., 2000). It follows that the maximal rectangles can be easily obtained by finding such isolated points.

We then select the optimal rectangles and consider that each of them is an equivalent representation of an association rule whose head is a class label (e.g., SF, NAC, or AC). Such rules are used to build our classifier.

The steps we follow in order to extract the association rules from the EEG data and to classify a patient's state are exemplified in the next section.

5.2 Rule Extraction and Classification

For the sake of clarity, we describe the adopted procedure by referring to a toy example where the data used as training set refers to nine patients (three for each class).

Step 1: Feature extraction. Consider the patients' raw EEG samples that are available as training set. We first extract features from the collected EEG samples, using the TD-FE or FD-FE schemes presented in Section 4. As an example, Fig. 5 illustrates the features obtained

	B1	B2	B3	B4	B5	B6	B7	B8	B9	B10	B11	B12	B13	Label
	Mean	waveLen	Variance	Auto-regression										
O1	33.954	-4	1860.9	1	-1.8722	1.0928	0.077665	-0.3711	0.20731	-0.05765	-0.26447	0.54903	-0.31912	Class Healthy
O2	37.362	41	2232.3	1	-1.3363	0.61118	0.64312	-0.29699	-0.26452	0.22298	0.034699	-0.06419	0.005384	Class Healthy
O3	42.011	28	2778.6	1	-1.5841	0.5435	0.54898	-0.39885	-0.2466	0.24142	0.016015	0.01941	-0.09515	Class Healthy
O4	53.58	-21	4622.7	1	-1.7226	0.58155	0.50927	-0.3617	-0.28726	0.38268	0.006498	-0.17789	0.086971	Class Non-active
O5	52.396	21	4615.8	1	-1.8318	0.73531	0.39856	-0.29223	-0.0961	0.16485	-0.18752	0.21037	-0.09022	Class Non-active
O6	51.404	42	3187.4	1	-1.5447	0.60515	0.41231	-0.26634	0.01629	-0.01061	-0.08779	0.23703	-0.14584	Class Non-active
O7	97.287	-193	15377	1	-2.0392	1.2561	0.26063	-0.61384	-0.0432	0.35107	-0.02676	-0.21225	0.12005	Class Active
O8	140.7	-311	38278	1	-2.2408	1.6277	0.10895	-0.64396	0.005835	0.37968	-0.15715	-0.11325	0.08825	Class Active
O9	168.15	-334	46189	1	-2.3581	1.8027	0.10798	-0.76958	0.022686	0.413	-0.08415	-0.23024	0.13719	Class Active

Fig. 5. Step 1: EEG time-domain features computed over the data of nine patients belonging to the three classes, namely, SF, NAC and AC.

	B1	B3	B6	B8	
	Mean	Variance	Auto-regression		
O1	0.2019269	0.0402888	0.60620181	0.48221108	Class Healthy
O2	0.2221945	0.0483297	0.33903589	0.3859118	Class Healthy
O3	0.2498424	0.0601572	0.30149221	0.51826971	Class Healthy
O4	0.3186441	0.1000823	0.32259943	0.46999662	Class Non-active
O5	0.3116027	0.0999329	0.40789371	0.3797266	Class Non-active
O6	0.3057032	0.0690078	0.33569091	0.34608488	Class Non-active
O7	0.5785727	0.3329148	0.69678815	0.79762988	Class Active
O8	0.8367529	0.8287255	0.90292339	0.83676811	Class Active
O9	1	1	1	1	Class Active

Fig. 6. Step 2: Transformation of EEG time-domain features into fuzzy binary relation.

	B1	B3	B6	B8	
	Mean	Variance	Auto-regression		
O1	0	0	1	1	Class Healthy
O2	0	0	1	1	Class Healthy
O3	0	0	1	1	Class Healthy
O4	1	0	1	1	Class Non-active
O5	1	0	1	1	Class Non-active
O6	1	0	1	1	Class Non-active
O7	1	1	1	1	Class Active
O8	1	1	1	1	Class Active
O9	1	1	1	1	Class Active

Fig. 7. Steps 3 and 4: Transformation of fuzzy binary relation into a crisp relation with $\alpha = 0.3$, and identification of optimal rectangles (highlighted in colors).

when the TD-FE technique is applied. These features are computed using equations (1)-(4) over the data of nine patients belonging to three classes of EEG data, namely, SF, NAC and AC.

The features are then assessed and selected. We do so by calculating the correlation of these features with the different patient classes: the features that are highly correlated with a class value (label), and low correlated with each other, are the most informative ones, and are thus selected.

Step 2: From feature values to fuzzy relation. In order to transform the selected features into a fuzzy binary relation, negative feature values are multiplied by -1 and all values are normalized with respect to their maximum. The goal of the normalization is to map all selected features from Fig. 5 onto non-dimensional values within the $[0, 1]$ range. The result is reported in Fig. 6.

Step 3: From fuzzy to crisp. We then transform the resultant fuzzy binary relation into a crisp relation (see Definition 2), by properly setting the α parameter (see Fig. 7).

Step 4: Finding optimal rectangles. The crisp binary relation values are then decomposed into a set of optimal rectangles (see Definition 6), using the algorithm presented in (Khcherif et al., 2000) and discussed in the previous section. The result of this operation in our example is shown in Fig. 7, where we note that there is an optimal rectangle for each patient class.

Step 5: From rectangles to rules. Based on the identified rectangles, we derive a set of association rules that can be used to effectively detect the class to which patients belong (see Table 1). As mentioned above, in our example there are three optimal rectangles, one for each class. Given a rectangle, we create a rule whose head is given by the corresponding class label and the body is determined by the values taken by the selected features within the rectangle. For instance, looking at Fig. 7, if all the patient's features take the value 1 under the crisp relation, then the patient belongs to the AC class.

However, this turned out into low classification accuracy while differentiating between the two classes SF and NAC. To enhance our approach, we therefore leverage what we called *shadow concept*: we consider not only the feature values for which the relation R_α is equal to 1, but also the negation of the features, i.e., the feature values for which the relation is equal to 0. In this case, both the features and the negation of the features of an optimal rectangle yield the condition part (body) of the rule, while the class of the patient represents its consequent part (head of the rule). Accordingly, we obtain three association rules (one for each class), as shown in Table 1. For completeness, in Table 2 we also report the association rules that we obtain applying the same procedure but using FD-FE instead of TD-FE.

Step 6: Classification. The obtained association rules are used to build a classifier at the mobile edge (the PDA). They are therefore applied to the patient's data in order to detect his/her state. Recall that, based on the detected patient's state, the PDA can select the most appropriate transmission option.

With regards to classification, while applying the above procedure to our training and validation data set, we observed that the parameter α has a strong impact on the accuracy of the classification procedure. In order to ensure high performance, we therefore perform classification in two stages, each using a different value of α (namely, α_1 and α_2). At the first stage, we only differentiate between normal cases (class SF or NAC) and abnormal cases (class AC), using the value α_1. Then, if a normal case is detected, we move to the next stage, and, use α_2 to further differentiate between SF and NAC patients. We remark here that the values of α_1 and α_2 are obtained during an offline training phase using exhaustive search.

Table 1
Steps 5: Association rules extracted from the relation R_α of Fig. 7 (i.e., when TD features are used).

Rule	**Class**
If $B_1 = 0$ AND $B_3 = 0$ AND ($B_6 = 1$ OR $B_8 = 1$) Then Class Healthy	Class Healthy
else If $B_3 = 0$ Then Class Non-active	Class Non-active
else If $B_1 = 1$ AND $B_3 = 1$ AND $B_6 = 1$ AND $B_8 = 1$ Then Class Active	Class Active

Table 2
Association rules created using FD features.

Rule	**Class**
If (all selected features = 0) Then Class Healthy	Class Healthy
If (at least one feature = 1 AND one feature = 0) Then Class Non-active	Class Non-active
If (all selected features = 1) Then Class Active	Class Active

6 Data Transfer

We now address the third and last component of our epileptic seizure detection system: the transfer of the data related to the patient's state toward the MHC.

Once classification is performed at the PDA through SIC, the PDA sends both a disorder notification and high-intensive monitoring data to the MHC if an emergency (i.e., AC) is detected. Instead, it transfers a much smaller amount of data if a normal pattern is observed. In particular, the PDA saves energy, time, and memory space, by sending to the MHC compressed data for the NAC and by transmitting only the relevant features for the SF. In the following, we detail the adaptive mechanism we exploit for EEG data compression at the PDA.

Let us consider that, in the case of NAC, the PDA processes the EEG signal using the so-called threshold-based Discrete Wavelet Transform (DWT) (Awad, Mohamed, El-Sherif, & Nasr, 2014), and that a Daubechies wavelet family is selected for this purpose (Hussein, Mohamed, & Alghoniemy, 2015b). Given signal x, we can write: $x = \Psi\alpha_w$ where Ψ is the Daubechies wavelet family basis and α_w is the vector of wavelet domain coefficients [2]. Such coefficients are then filtered using a filter with length $F = 2\kappa$, where κ is the order of the selected wavelet family. The longer the filter length, the higher the number of output coefficients. Next, according to the threshold-based DWT, the filtered coefficients that are below a predefined threshold are zeroed (Mallat, 2008). It follows that the number of output samples generated from the threshold-based DWT, hence the compression ratio, can be controlled by properly setting F as well as the value of such threshold. Indeed, the compression ratio (expressed as percentage) is given by:

$$C = \left(1 - \frac{M}{N}\right) \times 100 \tag{5}$$

where M is the number of output samples generated after the threshold-based DWT, and N is the length of the original signal. The encoding distortion caused by the compression can then be measured by the percentage Root-mean-square Difference (PRD) between the recovered EEG data and the original one, as

$$D = \frac{\|x - \hat{x}\|}{\|x\|} \cdot 100, \tag{6}$$

where x and $\hat{x}$ are the original and the reconstructed signal, respectively.

[2] Note that, in the case of multistage DWT, these coefficients are calculated recursively on multilevel wavelet decomposition.

Our experimental results, depicted in Fig. 8, confirm that the main parameters affecting the encoding distortion are the wavelet filter length (F) and the threshold value. The plot shows both the compression ratio and the distortion that are obtained by varying the two parameters. As mentioned, given F, the higher the threshold, the larger the number of samples that are zeroed, hence the higher the compression ratio. The reduced amount of data to be transmitted clearly translates into a lower energy consumption but at the expense of an increased distortion. When we fix the threshold value, an increasing F (i.e., a higher order of the Daubechies wavelet family) leads to a larger number of output samples and a more detailed representation of the signal, which reduces distortion. Interestingly, when the threshold value is small, the compression ratio grows quite noticeably with increasing F since the generated coefficients exhibit a smaller value and are therefore zeroed when thresholding is applied (see the green curves in Fig. 8). The price to pay for such better performance is an increased computational complexity. These trends are in agreement with the well-known fact observed in practical system design: there is always a tradeoff among energy consumption, system complexity and encoding distortion. Importantly, our adaptive compression technique enables the PDA to establish the preferred tradeoff by properly adjusting the encoder parameters, namely, F and the threshold value.

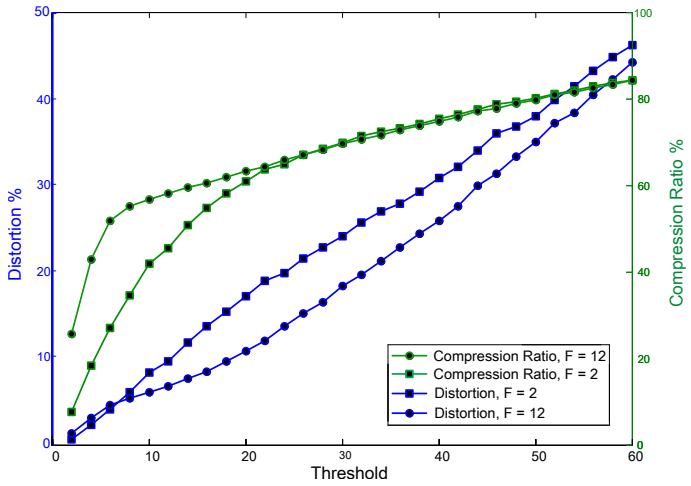

Fig. 8. Distortion versus compression ratio. Different values of filter length (i.e., Daubechies wavelet families) are considered.

7 Real-Time System Implementation

In this section, we present our implementation framework of a reliable energy-efficient EEG telemonitoring system. The main components and functionality of the implemented framework (see Fig. 9) can be summarized as follow:

Data Source (i.e., Emulator). This module is responsible for acquiring and sending the EEG signals to the PDA. Specifically, we focus on epileptic seizure detection leveraging the EEG dataset in (Andrzejak et al., 2001). Thus, every 200 msec, the Emulator sends a "Medical Record" to the PDA, i.e., our application-based packet. Each record contains 4096 EEG samples.

PDA (i.e. smartphone). It is responsible for communicating with the Emulator, receiving and processing the data and forwarding the processed/compressed data to a health monitoring server. The communication between the PDA and the server is performed through WiFi fol-

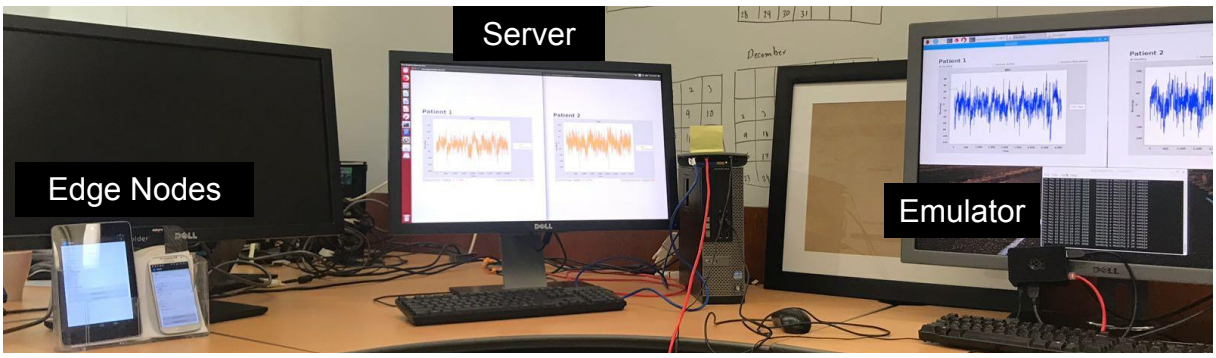

Fig. 9. The implemented system for EEG telemonitoring.

lowing the IEEE 802.11 (WiFi) standard (IEEE, 2007). In general, for a good interpretation of EEG data, large amount of data have to be gathered, analyzed, and transmitted to the remote server, which imposes a significant load on the PDA in terms of energy consumption, latency, and cost. Thus, performing in-network feature extraction, classification, and adaptive compression on the acquired data from Emotiv headset before transmission is essential. In this context, we have developed and implemented an Android application at the PDA (see Fig. 11-(b)) that performs the following tasks:

- Swift classification using proposed SIC algorithm in order to classify the acquired EEG signals.
- Threshold-based DWT compression, where the appropriate threshold can be adjusted based on the patient's state, desired compression ratio, application distortion threshold, and available energy budget. For implementing the DWT compression, we used the JWave library (i.e., a Java implementation of wavelet transform algorithms (Scheiblich, 2018)).
- Energy-efficient transmission, where the PDA decides to send to the remote server raw data, the extracted features (i.e., time features or frequency features), or compressed data, according to the detected state, while sending an emergency notification for the patients with abnormality.

Once the PDA receives a new medical record from the Emulator, it extracts the medical data and performs the aforementioned tasks. Then, it packages the processed data with the appropriate meta-data to create a new medical record shown in Fig. 10. This medical record contains: i) Patient ID, to support multiple patients, (ii) sequence number, i.e., unique data identifier, (iii) Modality, in case of considering multiple modality data, (iv) TimeStamp, for delay calculation, (v) isRaw?, to indicate if the transmitted data is raw or processed data, (vi) Medical Data (the processed EEG data), i.e., raw data, time/frequency features, or compressed data. Finally, the PDA send the created medical record to the health monitoring server through WiFi.

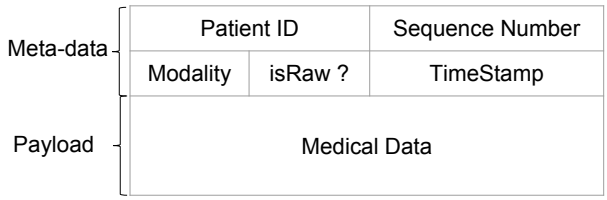

Fig. 10. Transmitted Medical Record from the Emulator.

Health monitoring server. A server application is developed to receive the transmitted data from PDA, then it performs: (i) data analysis and classification if it receives raw data; (ii) classification if it receives time/frequency features; (iii) data reconstruction, distortion evaluation, and classification if it receives compressed data. The developed applications at the Emulator,

PDA, and health monitoring server are shown in Fig. 11

We remark here that the proposed EEG telemonitoring system allows remote real-time monitoring of patients without constraining their activities. Thus, the proposed system can be used in several healthcare scenarios, e.g., the users can be patients at home or in a hospital, workers in a factory, or sports players. Indeed, the collected data coming from different scenarios can be processed at the Edge according to the specific requirements of each scenario/application, hence providing ultimate flexibility, robustness, and quality of service.

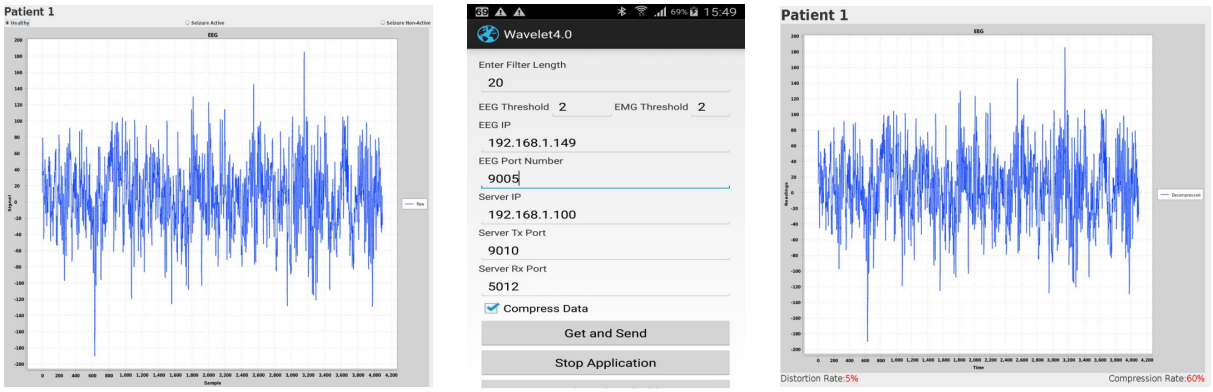

(a) (b) (b)

Fig. 11. Developed applications at: (a) Emulator, (b) PDA, and (c) health monitoring server.

8 Performance Evaluation

In this section, we investigate the performance of our s-health system using the implemented framework shown in Fig. 9. In the following, after presenting the experimental setup, we start by comparing the accuracy level of the classification outcome obtained at the server, when the different data reduction techniques are applied. Then, we focus on the performance of the proposed SIC scheme compared with different machine learning classifiers from the literature. Finally, we compare the performance of the implemented s-health system with a mobile-health monitoring system in terms of energy saving, battery lifetime, and delay reduction.

8.1 Experimental Setup

In the implemented monitoring system, a Samsung Galaxy S4 smartphone and a server desktop are used as a PDA and medical server, respectively, while the data source (*emulator*) is a Raspberry Pi. Since it is difficult to find a patient with seizures, we replaced the EEG headset with a raspberry Pi, which is used as a data emulator exploiting the EEG data set in (Andrzejak et al., 2001). The PDA is connected to both emulator and server via WiFi, where the three devices are connected to a dedicated private WiFi network using Cisco router. We limit the bandwidth on the server at a maximum rate of 4 Mbps using *wondershaper* application.

Our experiments start when the communication channels are established between the emulator, PDA, and server. Then, the medical records (Fig. 10) are generated from the emulator, and sent towards the edge node. Each medical record contains 4096 EEG samples and is 32 KB in size. The experiment ends when the server receives and acknowledges 18000 medical records.

We first consider the FD-FE technique and the classification accuracy (CA) that it can yield. In FD-FE, the EEG signal represented in the frequency domain is segmented into multiple sub-bands, each sub-band having a number of frequency components. Different subsets of these sub-bands can be selected as feature vector. Doing so we can control the amount of data corresponding to the selected features and, hence, the amount of transmitted data (see Table 3). Here we assume that each sample/frequency coefficient is represented by one byte.

Fig. 12 shows the ratio of the level of CA obtained with increasing features vector length, expressed in percentage. In general, the larger the amount of transmitted data, the higher the CA, except for some cases where the added sub-bands yield a performance decrease. The reason for this behavior is that, in some cases, the added data may "confuse" the classifier rather than help (see Table 3). On the contrary, with increasing length of the transmitted data, the consumed energy in the transmission process always increases. Thus, an optimal tradeoff between classification accuracy and energy consumption can be established, based on the application's requirements, patient's state, and energy availability at the PDA.

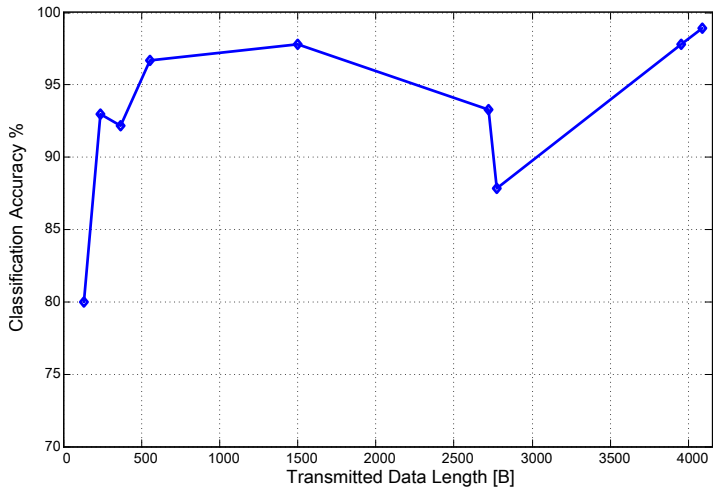

Fig. 12. Frequency-domain feature extraction: classification accuracy as the length of transmitted data varies.

The comparison among different data reduction techniques including TD-FE, FD-FE, downsampling (where the EEG sampling rate f_s varies), and the proposed adaptive lossy compression is presented in Table 4. In the case of data compression, we present the reduction in CA compared to the case of no compression (i.e., when raw data is transmitted), which yields a CA equal to 86.67%. Note that classification based on raw data in general leads to worse performance than in the case where TD or FD features are used. The reason is again that too much redundant information may mislead the classifier rather than improve its accuracy.

We observe also that the higher the sampling rate (i.e, number of sensed EEG samples per second), the larger the amount of transmitted data and the higher the accuracy. The only remarkable exception is represented by TD-FE: in this case (i) the amount of transmitted data does not depend on the sampling rate and (ii) we can achieve an accuracy of 95.56% while transmitting only 13 bytes instead of 4096. When, instead, compressed data is sent by the PDA to the MHC, increasing the compression ratio leads to a slight decrease in the CA with respect to the case where raw data is transferred, while significantly reducing the amount of transmitted

Table 3
Selected sub-bands and corresponding amount of transmitted data

Frequency sub-bands					**Transmitted data**
γ	β	α	θ	δ	**length [B]**
0	0	0	0	1	133
0	0	0	1	0	236
0	0	0	1	1	369
0	0	1	1	1	557
0	1	1	1	1	1501
1	0	0	0	1	2719
1	0	1	0	0	2774
1	1	1	1	0	3954
1	1	1	1	1	4087

data. Seemingly to the effect of increasing the compression ratio, lowering f_s decreases the length of transmitted data at the expense of a reduced CA. However, it is worth noticing that in some cases a higher compression ratio, or smaller f_s, still yields satisfactory values of CA. The reason is that, in such cases, the missed data is actually redundant thus not beneficial in terms of CA.

At last, comparing FD-FE to TD-FE and data compression, we observe that FD-FE can provide the best CA while offering significant flexibility in terms of data length: by properly selecting the subset of frequency sub-bands, the desired tradeoff between amount of transmitted data and CA can be easily obtained. However, while data compression still allows signal reconstruction at the MHC, FD-FE as well as TD-FE are irreversible: the original EEG signal cannot be reconstructed from its features, which may not be acceptable for some applications.

Table 4
Classification accuracy using compressed data relative to transferring raw data (which yields CA=86.67%), downsampling, frequency-domain features, and time-domain features

Compressed data length [B]	**Loss in CA [%]**	**Data length [B] /f_s [sample/s]**	**CA [%]**	**FD-FE length [B]**	**CA [%]**	**TD-FE length [B]**	**CA [%]**
4096	0	4096/128	86.67	4087	98.89	13	95.56
2384	3.3	2048/64	86.67	3954	97.78	13	95.56
1601	1.17	1024/32	84.33	1501	97.78	13	95.56
1239	0.9	819/25.6	81.33	557	96.67	13	95.56
819	2.37	682/21.3	85.67	236	93.3	13	95.56
645	1.67	585/18.3	86.3	133	80.3	13	95.56

8.3 Classification Evaluation

We now focus on the performance of the proposed SIC algorithm, and illustrate the effect of the α-cut on the obtained CA at the PDA level. We evaluate the performance of our SIC

algorithm when TD-FE and FD-FE are applied. Recall that for SIC-TD we use the TD-FE scheme presented in Section 4.1 and the association rules described in Table 1, while for SIC-FD, we use the feature extraction technique introduced in Section 4.2 and the association rules presented in Table 2. Also, we remark that, when working in the frequency domain, we get a much longer feature vector than in the case of TD-FE. Thus, for the sake of fairness, for FD-FE we apply the association rules only to the first 10 features.

Fig. 13 depicts the obtained CA as the value of α varies, for the three EEG classes (i.e., SF, NAC, and AC). Herein, we classify all 300 subjects by running the procedure only once (one-stage procedure). Also, we evaluate the CA of the proposed SIC algorithm with different machine learning classifiers, including random decision forests (RandomForest), Naive Bayes (NaiveBayes), k-Nearest Neighbors (IBk), and classification/regression trees (REPTree). Each of these classifiers is run using the default configuration in WEKA software with 5-fold cross-validation (Aksenova, n.d.). In SIC, when α is small, most of the obtained normalized features are equal to 1, while at high values of α, most of the obtained features are equal to 0. In both cases, our classifier cannot accurately differentiate between the patients' classes. In the middle region, when α ranges between 0.1 and 0.4, the value of the obtained features starts to vary between 1 and 0, which helps the SIC classifier to discriminate between different classes yielding a high accuracy. The best performance is obtained with SIC-TD and for α around 0.3, which corresponds to a CA of 82%. With SIC-FD, the best α is 0.27 leading to a CA of 64%. As mentioned, we found that Class SF and NAC exhibit many similarities, which result in a relatively low CA while trying to discriminate between these two classes. Thus, in order to enhance the performance of the SIC algorithm, we switch to a two-stage classification process that allows us to select two different values of α (namely, α_1 and α_2). The results for the SIC algorithm are depicted in Fig. 14 and Fig. 15.

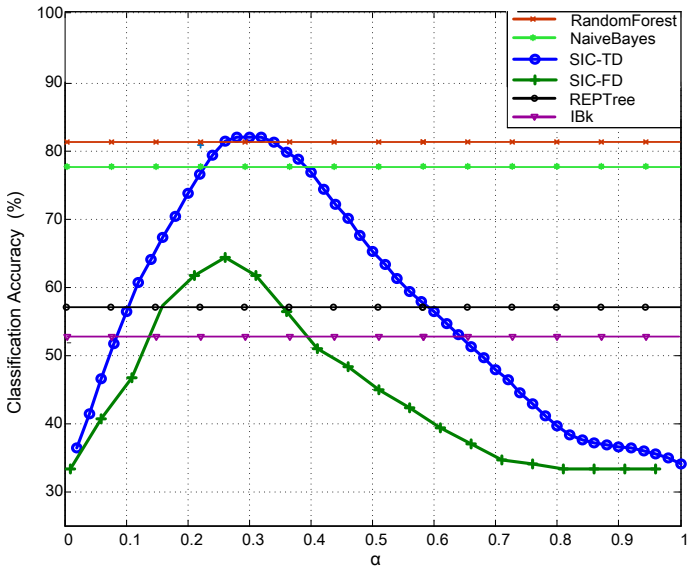

Fig. 13. Impact of α on the classification accuracy, for the three EEG classes.

In particular, Fig. 14 shows the results of the first classification stage as α_1 varies. In this stage, we classify the patient's state as normal and abnormal based on the observed EEG pattern. The former corresponds to class SF and NAC while the latter to class AC. The optimal value of α_1 for SIC-TD is now around 0.21 with CA equal to 98.3%, while it is 0.17 with a CA of 83% for SIC-FD.

For normal EEG patterns, we then proceed with the second stage using α_2 so as to achieve high CA between the SF and the NAC class. As shown in Fig. 15, in this case the optimal α_2 is 0.36 (with CA 80%) and 0.27 (with CA 75%) for SIC-TD and SIC-FD, respectively.

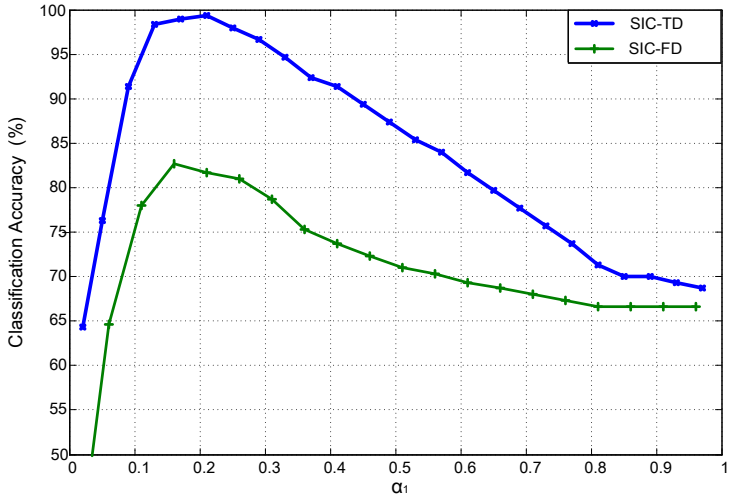

Fig. 14. Effect of varying α_1 on classification accuracy of normal/abnormal EEG patterns.

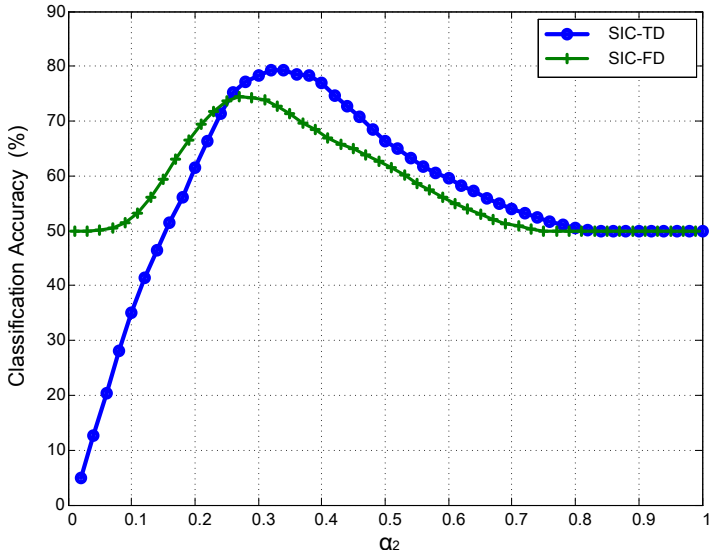

Fig. 15. Classification accuracy while discriminating between class SF and class NAC, as α_2 varies.

In conclusion, the advantages of the proposed SIC scheme are three-fold. First, its high classification accuracy and low complexity, which makes it amenable to be implemented in any smartphone or PDA. Second, in case of emergency, a quick emergency notification signal is triggered at the local processing unit (i.e., the PDA) as well as at the MHC, thanks to our swift classification technique. Third, in the case of normal EEG patterns, SIC can send only the EEG features thus saving a significant amount of energy at the PDA.

8.4 Energy and Delay Reduction

Here, we investigate the benefits of the proposed s-health system in terms of energy saving and delay reduction – indeed, reducing PDA's energy consumption due to continuous monitoring is one of the main objectives of this work. In particular, we compare the proposed s-health system

with the mobile-health monitoring system (m-health) and remote monitoring system (RM). M-health refers to a system that acquires and transmits EEG signals from wireless sensors to the PDA, which compresses and forwards the acquired data to the server/cloud. On the contrary, RM system conveys all processing and analysis tasks to the server, while a PDA is used as a communication hub that acquires and forwards the data from wireless sensors to the server (Menshawy et al., 2015). In these experiments, we analyze power usage and PDA's battery consumption using *Battery Historian* ("Analyzing Power Use with Battery Historian", 2018).

In Table 5, we conducted set of experiments considering a practical scenario where a PDA (i.e., smartphone) with full battery is running our monitoring application in parallel with the other default applications (e.g., Google services and Android system) until it runs out of battery. Also, it is assumed that 99% of the acquired EEG signals belong to SF, while 1% belong to AC. Table 5 show the percentile of battery consumption at the PDA due to the processing and transmission of our monitoring application, running time that PDA takes until it runs out of battery, and monitoring time which is the time of continuous monitoring (i.e., actual time of the sensed data sent from the emulator to the PDA).

These experiments demonstrate the efficiency of s-health and its scalability in increasing monitoring time compared to RM, while decreasing battery consumption with respect to both RM and m-health. Furthermore, leveraging the proposed s-health mitigates network overloading, hence, the monitoring time is almost the same as running time, This means that the PDA is able to continuously monitor patient's state during the whole run time. On the contrary, using RM and m-health (40%), there is a significant difference between monitoring time and running time due to the network congestion that results from continuously sending large volumes of data (see Table 5). Thus, the proposed s-health system has the ability to deal with a growing size of acquired data in an energy-efficient manner.

Table 5
PDA battery consumption and running time, as well as monitoring time of s-health, m-health (with $C = 40\%$ and $C = 60\%$), and RM systems.

Monitoring system	**Battery consumption [%]**	**Running time [hours]**	**Monitoring time [hours]**
RM	14.71	13.5	4.5
m-health (40%)	17.62	10	8.6
m-health (60%)	16.76	11.25	10.5
s-health	11.2	10.62	10.36

To further demonstrate the benefits of the proposed s-health system in terms of energy saving, Fig. 16 is presented. This figure assesses the performance of s-health, in terms of PDAs battery lifetime, compared to m-health (with $C = 40\%$) and RM. Note that, while obtaining these results, we set the compression ratio for s-health in case of NAC class to 40%, while considering that 10% of the acquired EEG signals belong to AC, 20% belong to NAC, and 70% belong to SF. Also, we considered the battery consumption due to our monitoring application only (neglecting battery consumption due to other running applications on the smartphone). Our results clearly show that s-health greatly outperforms RM and m-health with 60% and 30% extension in battery lifetime, respectively. We remark that the value of the compression ratio that we selected, represents a good tradeoff between transmission energy consumption and signal distortion (see Fig. 8). However, other values could be considered as well, depending on the

application requirements, patient's status, wireless channel conditions, and energy availability at the PDA.

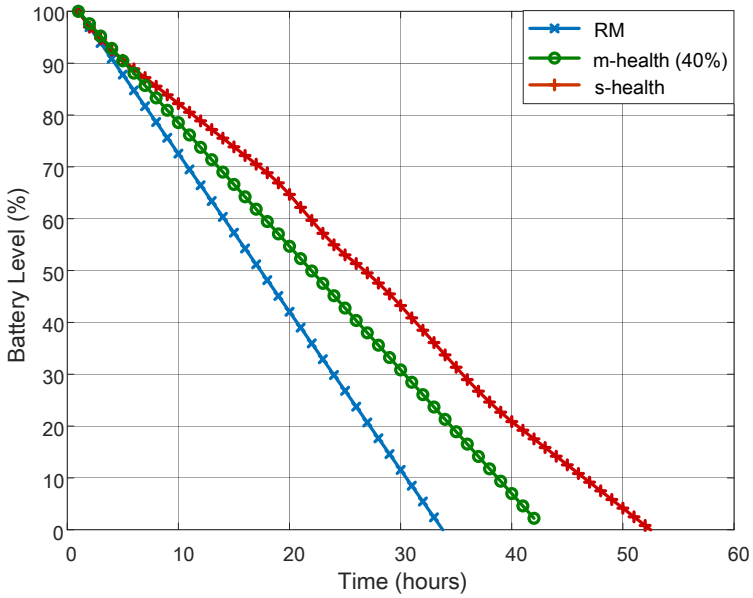

Fig. 16. Battery lifetime of s-health, m-health (with $C = 40\%$), and RM.

Finally, Fig. 17 demonstrates the benefit of s-health in reducing average transmission delay. Herein, transmission delay refers to the latency experienced by data from its receiving time at the PDA until its receiving time at the server. It is clear that reducing the amount of transmitted data to the server using s-health has a significant impact on avoiding network congestion, hence, decreasing average transmission delay by more than 90% with respect to RM.

We remark that the reduction in energy consumption and delay using s-health depends on the states of the patient, since in case of emergency (i.e., active seizures) the raw data should be sent to the MHC for intensive monitoring. However, the probability of AC is practically less than 1%, while seizures usually last for less than 3 minutes, after that the patient can turn to normal state for a long time before seizures coming back. Also, people who are more likely to have seizures and epilepsy (e.g., babies with abnormal areas in the brain, people with traumatic injury or serious brain injury, etc.) are usually put under monitoring after getting free of seizures for one to two years. In such cases, the proposed s-health system turns to be an effective solution for continuous monitoring of the patients' state in an energy-efficient manner and without limiting their daily activity.

9 Conclusion

In this paper, we investigated wireless EEG telemonitoring system and presented a full-fledged framework for seizures detection and notification. We presented a smart health monitoring system for detecting a patient's state that exploits feature extraction and fuzzy classification to provide high accuracy, while being suitable for implementation using mobile user devices. Then, depending on the patient's state, the proposed system can exploit different data reduction techniques, in order to reduce the amount of transmitted data. In particular, under normal patient's conditions, a significant amount of energy can be saved by transmitting properly compressed data, or by sending only the most representative EEG features that are pertinent

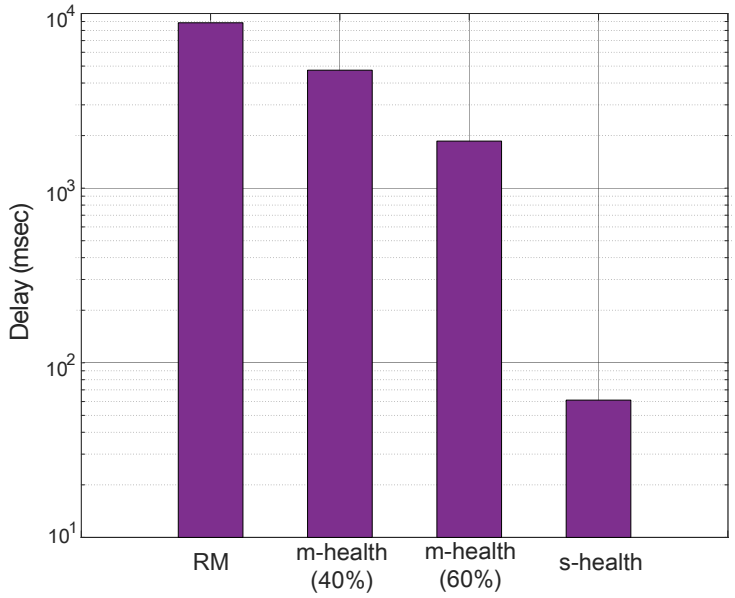

Fig. 17. Transmission delay of the s-health, m-health (with $C = 40\%$ and $C = 60\%$), and RM.

to seizures detection. Our results show that, in our system, time-domain feature extraction provides very high classification accuracy while minimizing the amount of transmitted data and energy consumption at the PDA. In particular, the amount of transferred data can be reduced from 4096 to 13 samples per patient, while maintaining high seizures detection performance with a classification accuracy above 98%. Frequency-domain feature extraction, instead, exhibits high flexibility, yielding the best trade-off between accuracy and energy consumption. Finally, adaptive data compression is a very valuable option whenever more data is needed at the mobile health center for further processing: compared to transmitting raw data, it reduces energy consumption and, unlike feature extraction techniques, it enables signal reconstruction at the mobile health center. In addition to that, the proposed s-health system has proven its scalability and efficiency in handling large volumes of acquired data, extending battery lifetime by 60%, and decreasing average transmission delay by 90% with respect to conventional remote monitoring systems that ignore data processing at the edge.

We remark that the proposed system is data-specific. Hence, the obtained reduction in transmission delay and energy consumption depends on the characteristics of the acquired data. However, we argue that designing a smart system to be specific to a certain type of data is fully consistent with the nature of IoT devices, which mostly acquire one type of data.

In our future work, multi-radio and multi-technology Edge gateway can be considered to locally process data coming from various data sources. Such Edge gateway can leverage the available network resources across different radio access technologies in order to increase the efficiency and scalability of the developed smart system.

Acknowledgment

This work was made possible by GSRA grant # GSRA2-1-0609-14026 from the Qatar National Research Fund (a member of Qatar Foundation). The findings achieved herein are solely the responsibility of the authors.

References

Adeli, H., Ghosh-Dastidar, S., & Dadmehr, N. (2007, Feb). A wavelet-chaos methodology for analysis of EEGs and EEG subbands to detect seizure and epilepsy. *IEEE Transactions on Biomedical Engineering*, *54*(2), 205-211.

Ahirwal, M. K., & londhe, N. D. (2012, March). Power spectrum analysis of EEG signals for estimating visual attention. *International Journal of Computer Applications*, *42*(15), 34-40.

Aksenova, S. S. (n.d.). Weka explorer tutorial. *School of Engineering and Computer Science California State University*.

Al-Dmour, J. A., Sagahyroon, A., Al-Ali, A., & Abusnana, S. (2017, Nov.). A fuzzy logicbased warning system for patients classification. *Health Informatics Journal*, 1-21.

Alja'am, J. M., Jaoua, A., Hasnah, A., Hassan, F., Mohamed, H., Mosaid, T., ... Cherif, H. (2006). Text summarization based on conceptual data classification. *International Journal of Information Technology and Web Engineering*, 22-36.

Alsheikh, M. A., Lin, S., Niyato, D., & Tan, H. P. (2014, Fourthquarter). Machine learning in wireless sensor networks: Algorithms, strategies, and applications. *IEEE Communications Surveys Tutorials*, *16*(4), 1996-2018.

Analyzing power use with battery historian. (2018, April). In *https://developer.android.com/topic/ performance/power/battery-historian.html, last visited.*

Andrzejak, R., Lehnertz, K., Rieke, C., Mormann, F., David, P., & Elger, C. (2001). Indications of nonlinear deterministic and finite dimensional structures in time series of brain electrical activity: Dependence on recording region and brain state. *Phys. Rev. E, 64, 061907, (2001).*

Awad, A., Mohamed, A., El-Sherif, A. A., & Nasr, O. A. (2014, December). Interference-aware energy-efficient cross-layer design for healthcare monitoring applications. *Comput. Netw., vol. 74*, 64-77.

Berg AT, Shinnar S, Levy SR, Testa FM, Smith-Rapaport S, Beckerman B, & Ebrahimi N. (2001). Two-year remission and subsequent relapse in children with newly diagnosed epilepsy. *Epilepsia*, *42*(12), 1553-1562.

Castanho, M., Hernandes, F., R, A. D., Rautenberg, S., & Billis, A. (2013, February). Fuzzy expert system for predicting pathological stage of prostate cancer. *Expert Systems with Applications*, *40*(2), 466-470.

Cerina, L., Notargiacomo, S., Paccanit, M. G., & Santambrogio, M. D. (2017). A fog-computing architecture for preventive healthcare and assisted living in smart ambients. In *2017 ieee 3rd international forum on research and technologies for society and industry (rtsi)* (p. 1-6).

Cosenza, B. (2012). Off-line control of the postprandial glycemia in type 1 diabetes patients by a fuzzy logic decision support. *Expert Systems with Applications*, *39*(12), 10693-10699.

Dastjerdi, A. V., & Buyya, R. (2016, Aug). Fog computing: Helping the internet of things realize its potential. *Computer*, *49*(8), 112-116.

Dubois, D., & Prade, H. (2000). *Fundamentals of fuzzy sets* (first ed.). Springer Science & Business Media.

Englander, & Jeffrey et al. (2014). Seizures after traumatic brain injury. *Archives of physical medicine and rehabilitation*, *95*(6), 1223-1224.

Epilepsy detector application. (2017). *http://www.epdetect.com/*.

Helmy, A., & Helmy, A. (2015, Dec). Seizario: Novel mobile algorithms for seizure and fall detection. In *Ieee globecom workshops (gc wkshps)* (p. 1-6).

Hussein, R., Mohamed, A., & Alghoniemy, M. (2015a, Feb). Energy-efficient on-board processing technique for wireless epileptic seizure detection systems. In *International conference on computing, networking and communications (icnc)* (p. 1116-1121).

Hussein, R., Mohamed, A., & Alghoniemy, M. (2015b). Scalable real-time energy-efficient EEG compression scheme for wireless body area sensor network. *Biomedical Signal Processing and Control 19*, 122-129.

IEEE. (2007). wireless LAN medium access control (MAC) and physical layer (PHY) specifications. *IEEE Standard 802.11*.

Khcherif, R., Gammoudi, M. M., & Jaoua, A. (2000). Using difunctional relations in information organization. *Information Sciences 125*, 153-166.

Kraemer, F. A., Braten, A. E., Tamkittikhun, N., & Palma, D. (2017). Fog computing in healthcare–a review and discussion. *IEEE Access*, *5*, 9206-9222.

Maddouri, M., Elloumi, S., & Jaoua, A. (1998). An incremental learning system for imprecise and uncertain knowledge discovery. *Journal of Information Sciences 109*, 149-164.

Mallat, S. (2008). *A wavelet tour of signal processing* (Third ed.). Academic Press.

Menshawy, M. E., Benharref, A., & Serhani, M. (2015). An automatic mobile-health based approach for eeg epileptic seizures detection. *Expert Systems with Applications*, *42*, 7157-7174.

Novak, V. (1989). *Fuzzy sets and their applications*. Adam Hilger, Bristol.

Pace, P., Aloi, G., Gravina, R., Caliciuri, G., Fortino, G., & Liotta, A. (2018). An edge-based architecture to support efficient applications for healthcare industry 4.0. *IEEE Transactions on Industrial Informatics*, 1-1.

Patel, M., & Wang, J. (2010, February). Applications, challenges, and prospective in emerging body area networking technologies. *IEEE Transactions on Wireless Communications, VOL. 17, NO. 1*, 80 - 88.

Phinyomark, A., Limsakul, C., & Phukpattaranont, P. (2009). A novel feature extraction for robust EMG pattern recognition. *Journal of Computing*, *1*, 71-80.

Proakis, J. G., & Manolakis, D. G. (2007). *digital signal processing: principles, algorithms and applications* (Fourth ed.). Pearson Prentice Hall.

Rossi, L. A., Krishnamachari, B., & Kuo, C. C. J. (2016, May). Energy efficient data collection via supervised in-network classification of sensor data. In *International conference on distributed computing in sensor systems (dcoss)* (p. 33-42).

Sarfraz, M. (2005). *Computer-aided intelligent recognition techniques and applications* (second ed.). John Wiley & Sons.

Sarkar, S., & Misra, S. (2016). Theoretical modelling of fog computing: a green computing paradigm to support IoT applications. *IET Networks*, *5*(2), 23-29.

Scheiblich, C. (2018). *A discrete fourier transform (dft), a fast wavelet transform (fwt), and a wavelet packet transform (wpt) in java.* `https://github.com/cscheiblich/JWave`.

Sheng, Z., Mahapatra, C., Zhu, C., & Leung, V. C. M. (2015). Recent advances in industrial wireless sensor networks toward efficient management in IoT. *IEEE Access*, *3*, 622-637.

Tatari, F., Akbarzadeh, M., & Sabahi, A. (2012, December). Fuzzy probabilistic multi-agent system for breast cancer risk assessment and insurance premium assignment. *Journal of Biomedical Informatics*, *45*(6), 1021-1034.

Thurman et al. (2011). Standards for epidemiologic studies and surveillance of epilepsy. *Epilepsia*, *52*(7), 2-26.

Xu, B., Xu, L. D., Cai, H., Xie, C., Hu, J., & Bu, F. (2014, May). Ubiquitous data accessing method in IoT-Based information system for emergency medical services. *IEEE Transactions on Industrial Informatics*, *10*(2), 1578-1586.

Yazicioglu, R., Torfs, T., Merken, P., Penders, J., Leonov, V., Puers, R., ... van Hoof, C.

(2009). Ultra-low-power biopotential interfaces and their applications in wearable and implantable systems. *Microelectron. J.*, 1313-1321.

Yuce, M., Ng, S., Myo, N., Khan, J., & Liu, W. (2007). Wireless body sensor network using medical implant band. *J. Medical Systems*, *31*(6), 467-474.